

Frequency shifting of pulsed narrow-band laser light in a multipass Raman cell

R. Sußmann, Th. Weber, E. Riedle¹ and H.J. Neusser

*Institut für Physikalische und Theoretische Chemie, Technische Universität München,
Lichtenbergstrasse 4, W-8046 Garching, Germany*

Received 17 July 1991; revised manuscript received 1 October 1991

A multipass cell is described which allows efficient stimulated Raman frequency shifting for low pump laser intensities and low gas pressures. The latter is important for Raman shifting of narrow-band Fourier-transform limited light pulses ($\Delta\nu = 75$ MHz). It is shown that frequency broadening of the Raman shifted light can be largely avoided in the Dicke narrowing regime at low pressures. For 75 MHz pump pulses and an H_2 density of 2.5 amagat we found a negligible broadening to 90 MHz of the stimulated Stokes light. This is far below the value of 250 MHz expected from spontaneous emission. The narrow-band Stokes pulses achieved in CO_2 enabled us to measure the pressure shift coefficient ($-0.71 \times 10^{-2} \text{ cm}^{-1}/\text{amagat}$) of this gas. It is demonstrated, for the example of benzene, that our technique provides a very practical light source for high resolution molecular spectroscopy.

1. Introduction

The tuning range of narrow-band single-mode dye laser systems is limited by the wavelength range and efficiency of the dyes and the available pump laser frequencies. Therefore it is highly desirable to develop a technique for frequency shifting of narrow frequency light without loss of spectral selectivity. Stimulated Raman scattering (SRS) in high density gases is known to be a convenient technique for frequency converting tunable dye laser emission, but has so far been used only for broader bandwidths.

Until 1990, no successful attempt had been made to reduce the bandwidth of Raman shifted light to its physical limits [1,2]. For a pump laser with negligible linewidth, the bandwidth of the Raman shifted light is determined by pressure broadening in the high density regime of the gaseous Raman medium (H_2 : $\rho > 5$ amagat) and by Doppler broadening in the low density regime (H_2 : $\rho < 2$ amagat).

Dicke narrowing [3] is expected to lead to a nar-

rowing of the linewidth of the Raman transition below these limits in a specific density regime. This has been observed by stimulated Raman backward scattering in H_2 [4], in spontaneous Raman forward scattering [5], and with the method of stimulated Raman gain spectroscopy [6–8]. In H_2 a minimum spontaneous Stokes linewidth of 250 MHz was observed at a density of 2.5 amagat. Another narrowing process is caused by the Q-branch collapse (line mixing) phenomenon [9]. In the Raman ν_1 band of CO_2 , both narrowing processes occur in same density regime of about 0.3 amagat [10,11].

Efficient Raman shifting of laser light in *single-pass* cells requires pressures of several bar [12]. Due to their increased interaction lengths, *multi-pass* cells are advantageous because they reduce the SRS threshold pump power [13] and allow the pressure to be reduced to the narrowing regime. With this technique and a low pressure of 900 Torr, Saint-Loup et al. achieved a linewidth of 120 MHz (fwhm) at a Stokes conversion efficiency of about 12% in the Raman medium CO_2 [2]. However, no data are available for the most common Raman medium H_2 .

In this work a new multipass cell that produces a narrowing beyond the spontaneous linewidth in H_2 and beyond the ν_1 bandwidth in CO_2 [10,11] is de-

¹ Present address: Joint Institute for Laboratory Astrophysics, University of Colorado and National Institute of Standards and Technology, Boulder, CO 80309-0440, USA (1991–1992 visiting fellow).

scribed. For the first time a linewidth of the Raman shifted light of less than 100 MHz is obtained in H_2 .

2. Experimental apparatus

Our experimental setup for narrow-band stimulated Raman shifting is shown in fig. 1. A multipass unit was designed and constructed for Stokes and anti-Stokes shifting of the extremely narrow-band light of a pulsed amplified cw single mode dye laser in the Raman media H_2 (shift: 4155 cm^{-1}) and CO_2 (shift: 1388 cm^{-1}). The setup consists of a mode-matching telescope [14], the multipass optics and the gas cell. A lens is used to receive a collinear beam at the exit of the optics, and a dispersion prism separates the fundamental and the frequency-shifted light.

For the multipass optics the Herriot design [15] was chosen. It combines a long optical path length with periodic refocusing and therefore provides reasonable conversion efficiency for the given pump pulse energy of 4–5 mJ and the low gas densities necessary for the narrowing. In previous works on Raman shifting with multipass optics the mirrors were positioned inside the gas cell containing the Raman medium [2,13]. In this work we decided to place the mirrors outside. This resulted in simple manufacturing and handling and enabled us to optimize the operation parameters of the cell easily.

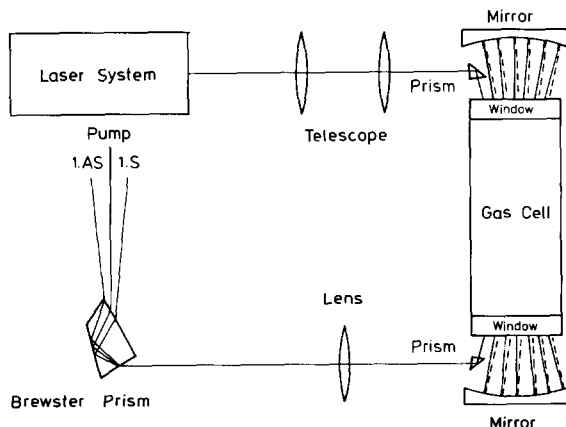


Fig. 1. Experimental setup for narrow-band Raman shifting. The mirrors of the multipass unit are placed outside the cell containing the gaseous Raman medium.

The inherent problems of this new design are additional losses and depolarization of the light at the windows of the intermediate gas cell [16]. In the small signal limit, the gain G in the Stokes output power due to the multipass arrangement is only dependent on the losses and the number n of passes through the gas cell [2,13]

$$G \approx (T_{\text{effS}})^{n-1} \frac{1 - (T_{\text{effP}})^n}{1 - (T_{\text{effP}})}, \quad (1)$$

with $T_{\text{effS,P}} = R_{S,P} T_{S,P}^2$. Here R_S and R_P are the mirror reflectivity and T_S and T_P the transmission of one cell window at the pump and Stokes wavelength, respectively. T_{effS} and T_{effP} represent the effective transmission for a single pass. Highly reflecting mirrors ($R_S \approx R_P \geq 99.5\%$) and antireflex coated windows with $T_S \approx T_P \geq 99.3\%$ yielded a multipass gain of $G=13$ for $n=26$ passes through the cell. Theoretically, a total cell transmittance of 60% is expected after 26 passes through the cell. The second inherent problem of our cell design is the strain birefringence of the pressure vessel windows. This causes a depolarization of the light, which strongly decreases the efficiency of frequency doubling necessary for an application in uv spectroscopy. The strain was controlled and minimized in an optical strain analyzing device.

Mode matching [14] fits the curvature of the wavefronts of the beam to that of the mirrors. Thus the spot radius on the mirrors (hwhm) w and the beam waist w_0 follow the equations [17]

$$w_0^2 = \frac{L\lambda}{\pi} \sqrt{\frac{1+g}{4(1-g)}}, \quad w^2 = \frac{L\lambda}{\pi} \sqrt{\frac{1}{1-g^2}}, \quad (2)$$

with $g \equiv 1 - L/R$. L is the distance between the mirrors of curvature R and λ the pump wavelength. Real and finite solutions for the spot radius w exist only if $0 \leq g^2 \leq 1$. From eq. (2) it can be seen that a nearly concentric geometry ($L/R \lesssim 2$) provides tightest focusing (thereby enhancing the Raman gain [13]). From eq. (2) it is also recognized that maximum w is obtained for ($L/R \lesssim 2$) and large cell dimensions (R, L), thus reducing the light intensity at the mirrors. Thus mirrors with $R=500\text{ mm}$ ($L \approx 950\text{ mm}$) were chosen, leading to a reasonable and convenient experimental setup and operating parameters well below mirror and cell window damage thresholds.

The beam of the pump laser is injected from one side of the multipass cell using a small adjustable right angle prism and leaves the cell on the other side by means of an identical prism (fig. 1). The light spots on the mirrors resulting from the different passes through the cell are located on a circle. Thus the spacing d between two neighboring spots must be larger than the size of the prism ($d > 3$ mm). Mirror substrates with 60 mm diameter are most suitable for these conditions, since $n=36$ is the number of passes that provides optimum gain in the small gain limit (eq. (1)) and thus an upper limit for efficient conversion in the high gain regime.

The gas cell was constructed to withstand pressures up to 7 atm with fused silica windows of 10 mm thickness ($\varnothing = 50$ mm). The cell length of 600 mm was chosen to be larger than twice the Rayleigh range ($z_R = 100$ mm) [17], where most of the conversion occurs.

The output of a single-mode cw dye laser (CR 699) was amplified in a three-stage amplifier to produce the narrow-band tunable pulsed laser light in the wavelength range 470–520 nm. The three amplifiers were pumped by the output of a XeCl excimer laser (EMG 150). At a wavelength of about 510 nm, light pulses of 5 mJ energy and 10 ns duration (fwhm) are produced from pump pulses of 100 mJ. Their

frequency width is about 75 MHz, and thus nearly Fourier-transform limited [18,19].

3. Experimental results and discussion

3.1. General operation conditions

In fig. 2a the dependence of the Stokes pulse energy E_S , measured for three different numbers of passes in CO_2 , is plotted as a function of the gas pressure. It may be seen that for a constant pump pulse energy ($E_P = 4.4$ mJ) the pressure needed to achieve a reasonable conversion efficiency can be significantly reduced for an increasing number of passes. The dashed horizontal line indicates the 7.5% conversion efficiency. For a pressure of 5 bar this conversion efficiency was obtained with 8 passes, for a lower pressure of 2 bar with 12 passes, and for the lowest pressure of 1.2 bar with 24 passes. It should be noted that the distance L between the mirrors has to be readjusted for each number of passes [2].

In fig. 2b the pulse energy of the first Stokes emission, E_S , is plotted as a function of the pump pulse energy, E_P , at a pressure of $p = 3$ bar. Here it is recognized again that the required pump pulse energy can be reduced when the number of passes through

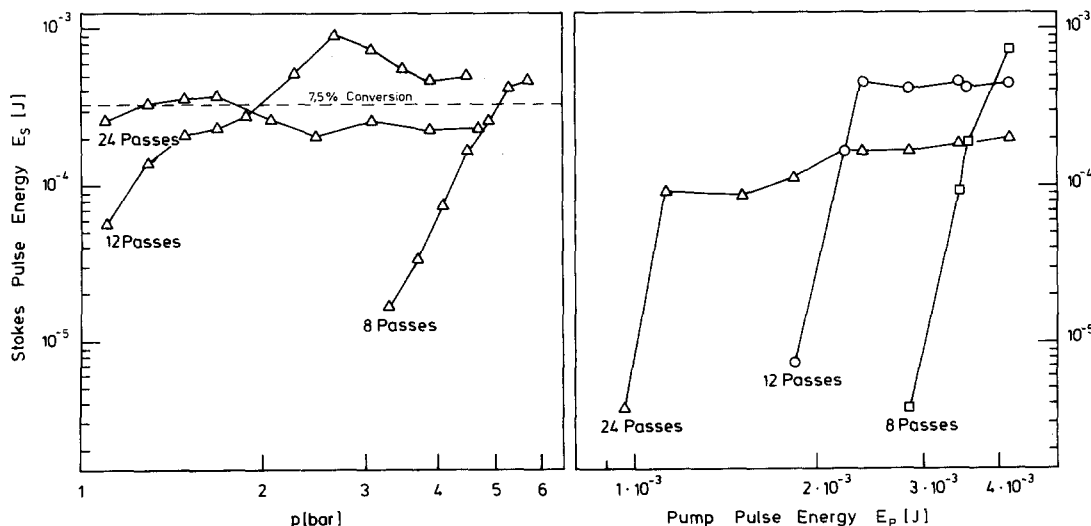


Fig. 2. Pulse energies E_S of first Stokes emission in CO_2 for various numbers of passes in the multipass cell as a function, (a) of the gas pressure p (constant pump pulse energy $E_P = 4.4$ mJ) and (b) of the pump pulse energy E_P (constant pressure $p = 3$ bar).

Table 1

Typical data of Stokes (S) and anti-Stokes (AS) shifting in CO₂ and H₂ with the multipass cell at low pressures: Raman pulse energy (E_R), pump pulse energy (E_P), conversion efficiency (E_R/E_P), wavelength of pump light (λ_P), wavelength of the Raman shifted light (λ_R) and its minimum linewidth ($\Delta\nu_{\min}$, fwhm). The pump laser linewidth is 75 MHz (fwhm).

		E_R (μJ)	E_R/E_P (%)	$\Delta\nu_{\min}$ (MHz)	λ_R (nm)	λ_P (nm)	Number of passes
H ₂ 3.5 amagat	1st S	1000	27.2	90(6)	647	485	12
	1st AS	38	1.0	100(20)	421	485	12
CO ₂ 0.9 amagat	1st S	455	16.0	117(21)	520	485	24
	2nd S	418	12.5	220(21)	594	510	24
	3rd S	327	9.8	–	647	510	26
	1st AS	64	2.8	146(23)	454	485	26
	2nd AS	12	0.4	–	447	510	28

the cell is increased. This means conversely that for a defined pump pulse energy the gain increases when the number of passes is increased. It will be shown below that this high gain is responsible for additional narrowing of the Stokes linewidth.

In order to achieve maximum conversion efficiency (table 1) of the Stokes and anti-Stokes shifted components of different orders, the number of passes had to be adjusted separately in each case. Typically, for CO₂ at the required low density of 0.9 amagat and a pump pulse energy of 3 mJ, conversion efficiencies of 16% for the first Stokes emission (24 passes) and 2.8% for the first anti-Stokes emission (26 passes) were achieved. Similarly, for an H₂ density of 3.5 amagat a high Stokes conversion efficiency of 27% and an anti-Stokes conversion efficiency of 1% were achieved in 12 passes.

3.2. Linewidth

The linewidth of the Raman Q₀₁(1) transition of H₂ in the Dicke narrowing regime has been investigated by spontaneous measurements [5] and by stimulated Raman gain spectroscopy [6–8]. The results [8] are in line with the relation

$$\Delta\nu_{\text{Dicke}} = \frac{D_0 k^2}{\pi\rho} + a\rho. \quad (3)$$

Here D_0 (1.39 cm² amagat/s) is the self-diffusion constant, k the difference vector between the wave vectors of the incident laser and emitted Stokes photons, and a (51.3 MHz/amagat) is the pressure-broadening coefficient. This relation is represented

by the solid line in the upper part of fig. 3a. It displays a minimum of the Raman linewidth of 250 MHz at a density of 2.5 amagat.

For comparison, in the lower part of the figure, the experimental results of this work are shown. They have been achieved by stimulated Stokes shifting in the multipass cell. The linewidth of both the pump and the Stokes light was measured with a high resolution confocal Fabry–Perot interferometer. Care was taken to maximize the pulse length of the Stokes light as to minimize its linewidth. Comparing the new results with the curve in the upper part of the figure reveals three striking differences.

(i) The minimum linewidth of 90 MHz achieved in SRS is significantly lower than the value of 250 MHz of the Q₀₁(1) transition [8] and is close to the exciting laser linewidth of 75 MHz; subtraction of the laser linewidth (assuming for simplification Lorentzian lines) would result in a linewidth of 15 mHz for the broadening caused by SRS in the multipass cell.

(ii) The linewidth minimum is shifted to higher densities (3.5–4 amagat).

(iii) The measured increase of the linewidth at higher densities (due to pressure broadening) is less than expected from spontaneous Raman data [5] and from stimulated Raman gain spectroscopy [8].

The effects described above for H₂ are also found for the Stokes-shifted SRS emission in CO₂ gas (fig. 3b, lower part). For comparison, the density dependence of the ν_1 full bandwidth of CO₂ measured by stimulated Raman gain spectroscopy [11] is shown in the upper part. Recently, the additional narrowing

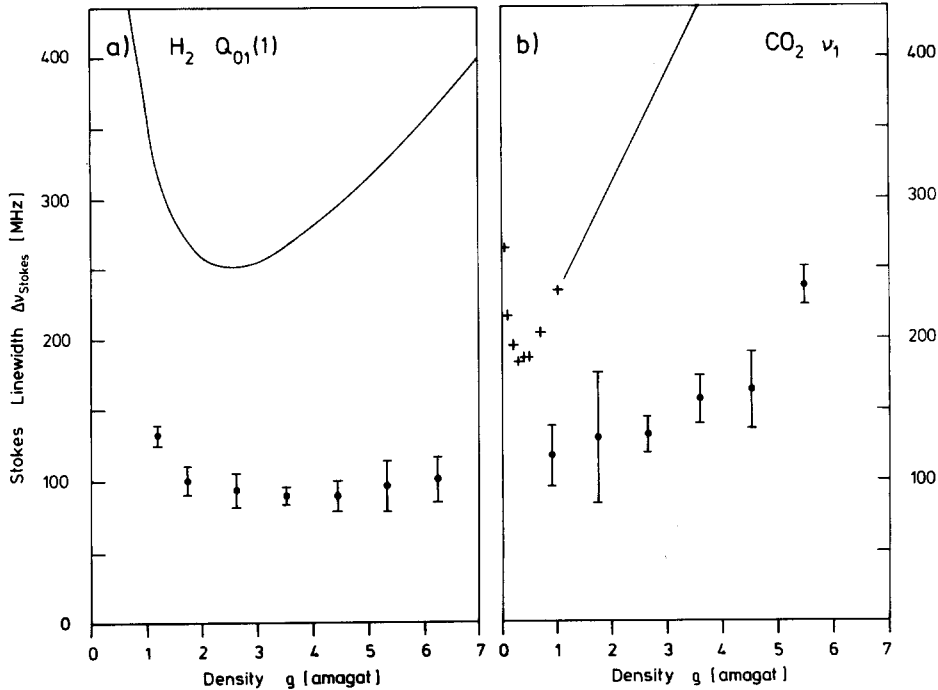


Fig. 3. (a) Upper part: theoretical dependence of the linewidth of the Raman $Q_{01}(1)$ transition in H_2 (eq. (3)) in good agreement with measurements of ref. [8]. Lower part: measured first Stokes linewidths for different gas densities in the multipass cell (this work). The error bars represent the accuracy of the frequency measurements and three standard deviations of the average value of several measurements. (b) Upper part: density dependence of the ν_1 full bandwidth of CO_2 measured by stimulated Raman gain spectroscopy (+) [11]; the solid line represents the linear pressure broadening. Lower part: measured first Stokes linewidths for different gas densities in the multipass cell (this work).

(i) of SRS was observed in CO_2 at a density of 1.2 amagat [20].

The effects (i)–(iii) are caused by the nature of the high gain stimulated Raman effect in the multipass cell leading to the well known gain narrowing phenomenon. Assuming a simple amplification model [17] the linewidths of the spontaneous and stimulated signals (assuming for simplification Lorentzian lines) are related by

$$\Delta\nu_{SRS} = \Delta\nu_{sp Em} \sqrt{\frac{\ln 2}{\ln(G_{SRS}/2)}}, \quad (4)$$

where G_{SRS} is the total Raman gain. For $G_{SRS} \sim e^{30}$ and $\Delta\nu_{sp Em} = 250$ MHz the minimum linewidth for H_2 eq. (4) yields $\Delta\nu_{SRS} \approx 38$ MHz. This is in reasonable agreement with the value of 15 MHz in our experiment. For broader laser linewidths and higher densities stronger narrowing than predicted by eq.

(4) has been observed in previous work [6,21]. With eq. (4) the results (ii) and (iii) can be explained by the higher gain expected for higher densities. Here gain narrowing becomes even more evident.

From figs. 3a and 3b it is seen that narrow-band Stokes–Raman shifting is possible at higher densities than predicted by spontaneous linewidth measurements (H_2 [5]) and stimulated Raman gain spectroscopy (H_2 [8], CO_2 [10,11]); similar results were found for anti-Stokes shifting (table 1). This is of great practical importance as it leads to a high conversion efficiency for the Raman shifted light.

3.3. Pressure shift

For the narrow-band Raman shifted light of the present work ($\Delta\nu = 90$ – 120 MHz, see table 1) the pressure shift in the Raman medium has to be considered. Using the multipass cell, the variation of the

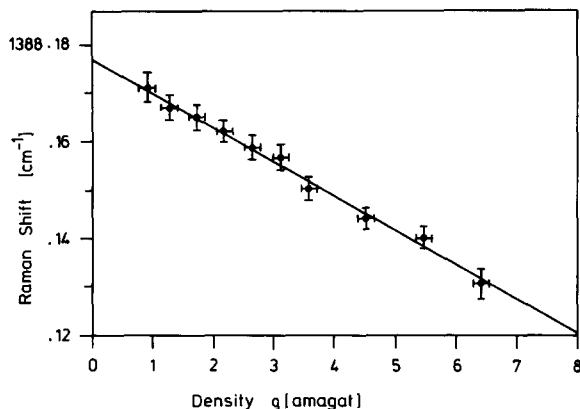


Fig. 4. Measured pressure shift of the Raman Stokes light of CO_2 . The solid line represents a linear least-squares fit to the experimental points, see eq. (5).

Raman frequency shift of the collapsed ν_1 Q-branch [10,11] as a function of the gas density was accurately determined for CO_2 gas, as shown in fig. 4. For absolute frequency calibration, the iodine absorption spectra were recorded [22] simultaneously, both in the frequency range of the fundamental laser and

the Stokes pulses. The measured Raman shift ν displays a linear dependence on the gas pressure and was found to follow the equation (solid line in fig. 4)

$$\nu = 1388.177(5) - 0.71(10) \times 10^{-2} \rho. \quad (5)$$

Here ν is the Raman shift in cm^{-1} and ρ the density in amagat.

4. Application to high resolution molecular uv spectroscopy

The Raman Stokes light, shifted in CO_2 gas, was frequency doubled and used for high resolution molecular spectroscopy in a supersonic beam. For demonstration the 6_1^0 hot band of benzene molecules is shown in fig. 5. It was measured with the technique of mass selected two-photon ionization via a resonant intermediate state [23]. Ionization was achieved by a second delayed frequency-doubled pulsed dye laser. For the experimental resolution of 160 MHz (see insert in fig. 5) most of the rotational lines in the vibronic 6_1^0 transition are resolved.

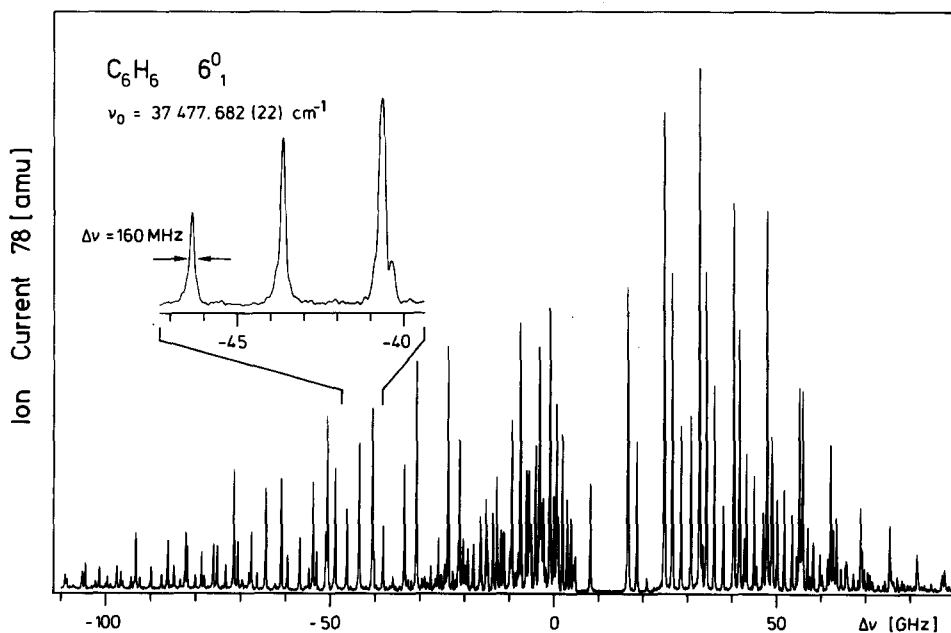


Fig. 5. Rotationally resolved spectrum of the 6_1^0 hot band of benzene C_6H_6 measured with the narrow-band Raman shifted Stokes light. For demonstration of the experimental linewidth a portion of the spectrum is shown on an expanded scale. For details, see text.

The high resolution and the good signal-to-noise ratio in the spectrum enabled us to determine the rotational constants B''_6 , C''_6 , B'_0 and C'_0 , the Coriolis coupling constant ζ''_6 and the band origin ν_0 with high precision on the basis of a symmetric top model [19]. A detailed description of this analysis will be given elsewhere, here only the results will be summarized briefly.

In a first step the ground state constant B''_6 was fitted to combination differences of lines with constant J' , K' , and ΔK but differing ΔJ . Next the constant C''_6 was calculated from the theoretically known rotational defect $\Delta = h/8\pi^2c(1/C - 2/B) = 0.0570$ amu \AA^2 for the 6_1 state [24]. Lastly, a fit of the remaining constants ζ''_6 , B'_0 , and C'_0 to 81 unblended lines was performed, yielding a standard deviation of 22.3 MHz. The results are

$$B'_0 = 0.181721 \text{ cm}^{-1}, \quad C'_0 = 0.090889 \text{ cm}^{-1},$$

$$B''_6 = 0.189721 \text{ cm}^{-1}, \quad C''_6 = 0.094830 \text{ cm}^{-1},$$

$$\zeta''_6 = 0.5829, \quad \nu_0 = 37477.68(2) \text{ cm}^{-1}.$$

The values of B'_0 and C'_0 represent the first direct determination of the rotational constants of the zero point S_1 state in benzene. They agree quite well with the values determined from the complex analysis of combination states in the S_1 state reported recently [25].

Acknowledgements

The authors are indebted to Professor E.W. Schlag for his continuous interest in the progress of this work. Financial support from the Deutsche Forschungsgemeinschaft and the Fonds der Chemischen Industrie is gratefully acknowledged.

References

- [1] J.C. White, Topics in Applied Physics, Vol. 59. Stimulated Raman scattering (Springer, Berlin, 1987) p. 115.
- [2] R. Saint-Loup, B. Lavorel, G. Millot, C. Wenger and H.C. Berger, J. Ram. Spectr. 21 (1990) 77.
- [3] R.H. Dicke, Phys. Rev. 89 (1953) 472.
- [4] P. Lallemand, P. Simova and G. Bret, Phys. Rev. Lett. 17 (1966) 1239.
- [5] J.R. Murray and A. Javan, J. Mol. Spectrosc. 29 (1969) 502.
- [6] J. Kleinschmidt, H.G. Walther and B. Wilhelm, Wiss. Ztschr. Friedrich-Schiller-Univ. Jena, Math.-Nath. R. 22 (1973) 287.
- [7] F. De Martini, F. Simoni and E. Santamato, Optics Comm. 9 (1973) 176.
- [8] A. Owyong, Optics Lett. 2 (1978) 91.
- [9] V.I. Alekseev and I.I. Sobel'man, Sov. Phys. JETP 28 (1969) 991.
- [10] R. Roy, D.S. Elliot, D. Meschede, F.M. Pipkin and S.M. Smith, Chem. Phys. Lett. 93 (1982) 603.
- [11] B. Lavorel, G. Millot, R. Saint-Loup and H. Berger, J. Chem. Phys. 93 (1990) 2185.
- [12] V. Wilke and W. Schmidt, Appl. Phys. 18 (1979) 177.
- [13] R. Trutna and R.L. Byer, Appl. Optics 19 (1980) 301.
- [14] H. Kogelnik and T. Li, Appl. Optics 5 (1966) 1550.
- [15] D. Herriot, H. Kogelnik and R. Kompfner, Appl. Optics 3 (1964) 523.
- [16] A. Owyong, Ch.W. Patterson and R.S. McDowell, Chem. Phys. Lett. 59 (1978) 156.
- [17] A.E. Siegman, Lasers (Oxford Univ. Press, Oxford, 1986).
- [18] E. Riedle, R. Moder and H.J. Neusser, Optics Comm. 43 (1982) 388.
- [19] E. Riedle, Th. Knittel, Th. Weber and H.J. Neusser, J. Chem. Phys. 91 (1989) 4555.
- [20] B. Lavorel, private communication.
- [21] V.A. Chirkov, V.S. Gorelik, G.V. Peregudov and M.M. Sushchinskii, ZhETF Pis. 10 (1969) 416.
- [22] S. Gerstenkorn and P. Luc, Atlas du spectre d'absorption de la molecule de l'iode (CNRS, Paris, 1978).
- [23] Th. Weber, A. von Bargaen, E. Riedle and H.J. Neusser, J. Chem. Phys. 92 (1990) 90.
- [24] M.F. Jagod and T. Oka, J. Mol. Spectrosc. 139 (1990) 313.
- [25] E. Riedle and J. Pliva, Chem. Phys. 152 (1991) 375.